LAWRENCE
LIVERMORE
NATIONAL
LABORATORY

LLNL-JRNL-663112

Catch and Release: Reaction Dynamics from a Freed "Tension Trapped Transition State"

J. Wang, M. T. Ong, T. B. Kouznetsova, J. M. Lenhardt, T. J. Martinez, S. L. Craig

October 22, 2014

Journal of Organic Chemistry

Disclaimer

This document was prepared as an account of work sponsored by an agency of the United States government. Neither the United States government nor Lawrence Livermore National Security, LLC, nor any of their employees makes any warranty, expressed or implied, or assumes any legal liability or responsibility for the accuracy, completeness, or usefulness of any information, apparatus, product, or process disclosed, or represents that its use would not infringe privately owned rights. Reference herein to any specific commercial product, process, or service by trade name, trademark, manufacturer, or otherwise does not necessarily constitute or imply its endorsement, recommendation, or favoring by the United States government or Lawrence Livermore National Security, LLC. The views and opinions of authors expressed herein do not necessarily state or reflect those of the United States government or Lawrence Livermore National Security, LLC, and shall not be used for advertising or product endorsement purposes.

Catch and Release: Reaction Dynamics from a Freed "Tension Trapped Transition State"

Junpeng Wang,[1] Mitchell T. Ong,[2] Tatiana B. Kouznetsova,[1] Jeremy M. Lenhardt,[3] Todd J. Martínez,*[,4] Stephen L. Craig*[,1]

[1]Department of Chemistry, Duke University, Durham, NC 27708

[2] Materials Science Division, Physical and Life Sciences Directorate, Lawrence Livermore National Laboratory, Livermore, CA 94550

[3]Chemical Sciences Division, Lawrence Livermore National Laboratory, 7000 East Avenue, Livermore, CA 94550

[4]Department of Chemistry, Stanford University, Stanford, CA 94305

Supporting Information Placeholder

ABSTRACT: The dynamics of reactions at or in the immediate vicinity of transition states are critical to reaction rates and product distributions, but direct experimental probes of those dynamics are rare. Here, *s-trans*, *s-trans* 1,3-diradicaloid transition states are trapped by tension along the backbone of purely *cis*-substituted *gem*-difluorocyclopropanated polybutadiene using the extensional forces generated by pulsed sonication of dilute polymer solutions. Once released, the branching ratio between symmetry-allowed disrotatory ring closing (of which the trapped diradicaloid structure is the transition state) and symmetry-forbidden conrotatory ring closing (whose transition state is nearby) can be inferred. Net conrotatory ring closing occurred in 5.0 ± 0.5% of the released transition states, as compared to 19 out of 400 such events in molecular dynamics simulations.

Introduction

Reaction dynamics in the vicinity of transition states are intrinsically tied to reaction mechanisms and product distributions. Understanding those dynamics, and if/how they are influenced by the trajectory that brought the molecule to that point, is therefore of significant interest. To that end, it is desirable to know the intrinsic dynamics of transition states – i.e., how a reaction proceeds if a molecule is dropped right at the transition state – and to compare observations to predictions based on molecular simulations and/or transition state theory. To date, the experimental observations of transition state structure and dynamics are based either on a characterization of product energy levels through scattering experiments, such as those performed by Polanyi[1] and Brooks,[2] the time-resolved pump-probe "femtochemistry" experiments pioneered by Zewail,[3] or the negative ion photodetachment experiments of Neumark[4] and Lineberger.[5] The dynamics in question tend to focus on a single trajectory as the activated complex descends toward product from either side of the (often symmetrical) dividing surface. Studies involving branching between non-degenerate pathways, for example those accessed through an additional dividing surface near that on which the activated complex resides, are rare.

In recent years, covalent mechanochemistry has been explored as a new methodology for studying reaction mechanisms.[6] To this end, various methods have been developed to probe force-coupled reactions,[7] including single-molecule force spectroscopy,[8-10] pulsed ultrasonication,[11] Boulatov's molecular probes,[12] and Matyjaszewski and Sheiko's bottle brush polymers.[13] Among these techniques, the use of pulsed sonication of polymer solutions is advantageous in that the experiments are operationally straightforward and the products of force-coupled reactions can be conveniently characterized by conventional spectroscopic techniques. During sonication, elongational flow fields are generated by cavitation, which includes the nucleation, growth and collapse of microbubbles.[14] A velocity gradient is then formed in the direction of a collapsing bubble; the polymer segments that are closer to the bubble have a higher velocity than those farther from the bubble,[14] and the polymer is thus stretched and elongated. The mid-chain the polymer is typically where the highest force is located and chain scission occurs.[8]

Sonicating mechanophore-embedded polymers provides an opportunity to probe the mechanochemical response of the molecules in solution, and we have recently used sonication to demonstrate the concept of tension trap-

ping,[15] in which transition states and high-energy intermediates are stabilized as global minima on force-coupled potential energy surfaces.[15] The force is delivered by overstressed polymer "handles," and tension trapping has been applied to carbonyl ylides[16] and to the 1,3-diradicaloid transition state of *gem*-difluorocyclopropane (*g*DFC) isomerization,[15] enabling unexpected isomerizations,[15,16] intermolecular chemical trapping of the dynamically trapped species,[15,16] and new, intramolecular reactions between multiple transition states trapped in proximity.[17]

Here, we use tension trapping to study the branching ratio between competing ring closing pathways following the release of the tension trapped 1,3-diradicaloid, which, as we have pointed out previously, corresponds to a transition state of force-free *g*DFC isomerization.[18] The majority of released diradicaloids proceed along one of two degenerate disrotatory pathways of which they are the transition state, essentially falling energetically downhill on either side of the dividing transition state surface. But a small fraction of the released transition states instead pass across an additional, higher-energy dividing surface that is not along the minimum energy pathway associated with the initial transition state. As a result, ~5% of the trapped diradicaloids, once released, ultimately close either via an orbital symmetry forbidden conrotatory pathway, or a monorotatory pathway followed by symmetry allowed disrotatory ring closing. A similar branching ratio is observed in molecular dynamics simulations.

Results

We reported previously that the force induced ring-opening of *cis*- and *trans*-*g*DFC under sonochemical conditions leads to tension trapping of a 1,3-diradicaloid that closes preferentially to the *cis*-*g*DFC once the tension is removed. Ring closing to the higher energy *cis*-*g*DFC isomer is kinetically favored because of the lower barrier for the symmetry-allowed disrotatory ring closing reaction relative to that of the symmetry-disallowed conrotatory reaction.[15] The orbital symmetry associated with *2,2*-difluoro-*1,3*-diyls has been previously characterized by Borden and co-workers,[19] and the 2 π-electron nature of the system is attributed to the electron withdrawing character of the fluorines. These ring closing dynamics lead to a counter-intuitive result: there is a net contraction in length along the affected regions of the polymer backbone in response to a force of tension (the polymer grows shorter once it is pulled), and the products are higher in energy than the reactants, as there is a net conversion of *trans*-*g*DFC to *cis*-*g*DFC.[15] It is clear from the prior studies that the vast majority of the released diradicaloids closed via a disrotatory motion, but we set out to quantify the small fraction of ring closing reactions that occurred via a net conrotatory motion, thus directly probing the reaction dynamics in the vicinity of the transition state dividing surface.

The experimental design is shown in Figure 1. Ring-opening metathesis polymerization[20] (ROMP) of difluorocyclopropanated cyclooctadiene **1** yielded *g*DFC polybutadiene (PB) **2**. The methodology gave a polymer

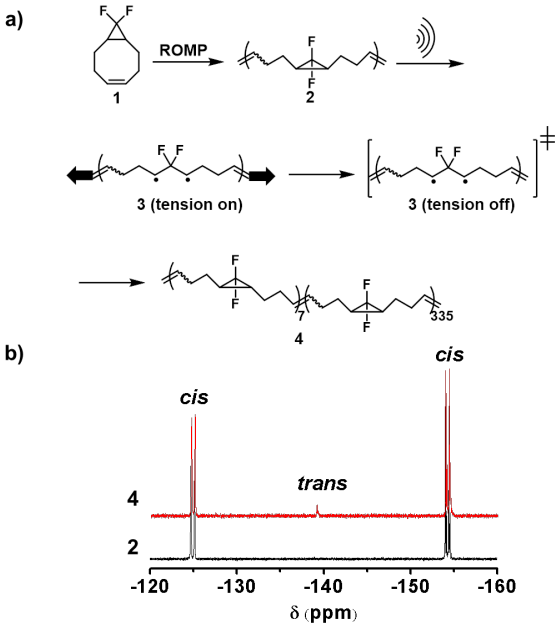

Figure 1. a) Ring-opening metathesis polymerization of **1** generates pure *cis*-*g*DFC-PB **2**, which was sonicated in dilute solution for 1 hour. When force is applied to **2**, diradicaloid transition state structures **3** are trapped under tension as global minima on the force-coupled potential energy surface. When the force is released, **3** is converted to a true transition state saddle point, and ring closure occurs rapidly in either a disrotatory or conrotatory manner to form copolymer **4**. **b)** ^{19}F-NMR of **2** (bottom, black) and **4** (top, red): the peaks at -125 ppm and -154 ppm correspond to *cis*-*g*DFC, while the peak at -139 ppm corresponds to *trans*-*g*DFC.

with only *cis*-connected *g*DFCs along its backbone, which allowed us to quantify the formation of very small levels of *trans*-*g*DFC that might have been obscured by the nascent *trans* content in previous studies.[15] Polymer **2** was then subjected to pulsed ultrasonication (30% amplitude, 11.9 W/cm^2), conditions previously shown to mechanically force the *g*DFCs open into trapped 1,3-diradicaloid transition states.[15] After 60 min of sonication, the molecular weight was reduced from 115 kDa to 54 kDa, and low levels (2%) of *cis*-to-*trans* isomerization were observed by ^{19}F NMR (**4**, Figure 1).

In order to occur in pulsed ultrasound, the timescale of a mechanochemical reaction must be comparable to, or shorter than, the timescale of the extensional flow event that generates the tension (~10^{-8} – 10^{-6} s).[21] Thus, the force-coupled activation energy for *cis*-to-*trans* *g*DFC isomerization under these conditions must be less than ~9 kcal mol^{-1}. Our calculations show that the force nec-

essary to lower the activation energy to this extent is also sufficient to stabilize the 1,3-diradicaloid as a global minimum on the force-coupled potential energy surface.[15] In other words, direct mechanochemical *cis*-to-*trans* isomerization is not possible in these experiments, and so when *trans*-*g*DFC is observed, it must have been formed from trapped transition states that close once the tension is released.

We can therefore quantify the number of disrotatory ring closing reactions, and so in order to quantify the probability of disrotatory closure, we need only to know how many 1,3-diradicaloids were trapped and subsequently released. Because most diradicals close back to the original *cis* configuration, direct measures of ring opening are not available. The extent of ring opening can be gauged fairly accurately by comparison to similar systems, in particular the mechanochemical ring opening of *gem*-dichlorocyclopropanes (*g*DCC).[22] Although the reaction outcomes are different, the activation energies and transition state geometries for *g*DCC and *g*DFC ring opening are similar, and the extents of sonochemical ring opening of the two *trans* isomers are indistinguishable.[23] In addition, we have recently found that the threshold forces for mechanochemical ring opening of *cis*-*g*DCC and *cis*-*g*DFC are very similar (in fact, closer than those of the corresponding *trans* isomers that are themselves effectively indistinguishable in sonication), as measured by single molecule force spectroscopy (timescale ~10 ms).[24] When the force-rate relationship derived from the force spectroscopy is extrapolated to the time scale of sonication (10^{-8} s), it is determined that the forces required to activate *cis*-*g*DFC is nearly indistinguishable from that required to activate *cis*-*g*DCC (2290 pN vs. 2370 pN, respectively; see Supporting Information).

We therefore synthesized a 123 kDa *cis*-*g*DCC-PB and subjected it to sonication conditions that are identical to those used for the *g*DFC-PB. The ring opening and molecular weight at different time intervals were characterized by ^{1}H NMR and gel permeation chromatography (GPC), respectively. As shown in Figure 2a, there is a linear relationship between *g*DCC ring opening and the scission cycle (*SC*, where $SC = \frac{\ln M_{n(0)} - \ln M_{n(t)}}{\ln 2}$. One scission cycle is the point at which the polymer M_n is cut in half, two scission cycles where it has been reduced to ¼ its initial value, etc…). The data are fit by the following line:

$$\text{Fraction of ring opening} = 0.51 \times SC \qquad (1)$$

The M_n of polymer **2** was therefore monitored as a function of sonication time, and the percentage of activated *g*DFC was estimated using eq. 1. The *trans*-*g*DFC content of the polymers increased linearly with scission cycle (Figure 2b), and the probability of net conrotatory ring closing is given by the ratio of the fraction of total rings that closed to *trans*-*g*DFC (from ^{19}F NMR) to the fraction of total rings that opened (from eq. 1). As shown in Figure 2b, the branching fraction remained constant (5.0 ± 0.5%) over the data reported.

a)

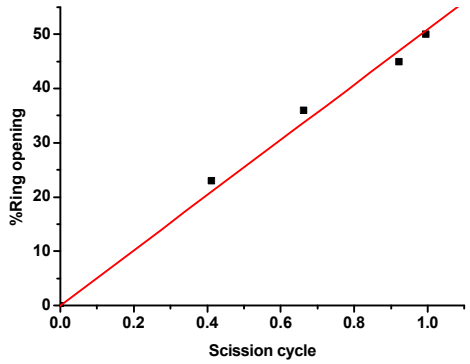

b)

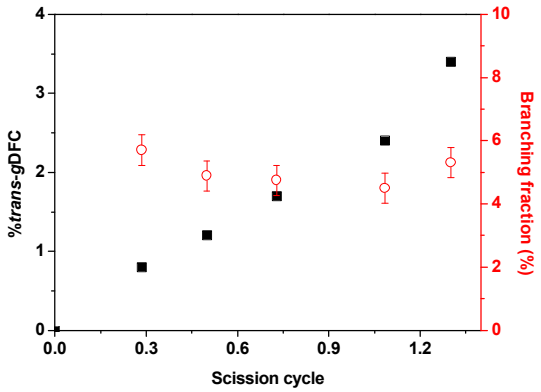

Figure 2. a) Sonication of *g*DCC polymer (1 mg/mL in THF, 6-9 °C, N_2 atmosphere). The ring opening percentage was characterized from ^{1}H NMR and plotted against scission cycle. **b)** Sonication of polymer **2** (1 mg/mL in THF, 6-9 °C, N_2 atmosphere). The percentage of *trans*-*g*DFC (black filled square, characterized from ^{19}F NMR) and branching fraction (red empty circle) were plotted against scission cycles. The branching fractions are determined from the ratio of the percentage of *trans*-*g*DFC to the percentage of the ring opening of *cis*-*g*DCC at certain scission cycles.

The fact that the branching fraction stays constant is significant, because a given *g*DFC can theoretically be activated multiple times. Of course, only the fate of the last ring opening/closing is reported, and since *trans*-*g*DFC is less reactive than the *cis* isomer,[24] it is possible for *trans*-*g*DFC to turn into a sort of kinetic sink as the original *g*DFCs undergo repeated activations. If such contributions were significant, they would be revealed

by an increase in the conrotatory branching fraction with reaction time. The fact that the branching fraction remained constant suggests that such contributions are not significant over the range of times employed, and so the branching fraction is indicative of the "true" branching fraction of the reactants. We note that with even longer sonication times, however, the branching fraction does start to increase as expected (see SI), but we rely on the data in the "constant branching fraction" time interval for our interpretation.

The overall *cis* to *trans* isomerization is caused by conrotatory ring closing or monorotation followed by disrotatory ring closing, meaning that 5.0 ± 0.5% of all released transition states undergo either conrotation or monorotation. The results and ensuing dynamical picture are summarized in Figure 3. We compared this result to that obtained from molecular dynamics simulations[25] on the parent *g*DFC diradicaloid,[15] trapped using simulated trapping forces of 2 and 3 nN and then released. A total of 400 trajectories were computed (200 each at 2 nN and 3 nN). We observed that 17 of the 400 trajectories closed in a direct symmetry forbidden conrotatory fashion, and an additional 2 of the 400 underwent net conrotatory ring closing via sequential monorotatation followed by disrotation. The total net conrotatory ring closing branching fraction of 4.75 ± 2% (19/400) is within statistical uncertainty of the experimental branching ratio.[3]

Discussion

The observed 19:1 branching ratio between the disrotatory and conrotatory pathways is smaller than that predicted by transition state theory for a difference in activation energies of 4 kcal/mol[15] (~1300:1 at 280 K). It is also smaller than the reported 107:1 ratio between *cis*-*g*DFC racemization and *cis*-to-*trans* isomerization observed in the thermally promoted stereomutations of *cis*-substituted *g*DFCs.[18] These observations are reminiscent of those noted previously by Carpenter in molecular dynamics simulations of the thermal interconversion of bicyclo[2.2.1]hept-2-ene.[26] In that case, the lifetime of the biradical intermediate showed a bimodal distribution; 10 of the 100 trajectories passed through the transition state and exited in 250 - 350 fs, whereas the rest failed to take the exit directly and their lifetime extended to 0.1 ns. The short-lived intermediates yielded only inversion product, and the long-lived trajectories formed both inversion and retention products in a ratio of 1:1. The difference in the product distributions was attributed to dynamic effects in the short-lived trajectories due to initial inertia.[26] Similar inertial effects could be at play for the force-free isomerization of *g*DFC: the inertia of disrotatory ring opening might channel the reactant towards a disrotatory ring closing process.[27] In the tension trapping experiments, however, the trapping would effectively negate any memory of the initial ring opening trajectory, so that conrotatory ring closing would be more prevalent than in the force-free case.

An alternative explanation involves the dynamics associated with the release of tension. The force does not instantaneously drop from that required for trapping (> 2 nN) to zero; there is a time scale associated with the disappearance of the force. A reasonable consideration, therefore, is how much force still remains on the system when the ring closure occurs, as that force could bias the ring closing outcome. The calculated force-modified potential energy surface for the perhydro-*g*DFC (see SI) shows that the observed disrotatory ring closing is favored only at low force. To have a selectivity of ~20:1 or greater, the activation energy for disrotatory ring closing needs to be at least ~2 kcal/mol lower than that for conrotatory ring closing. The disrotatory ring closing barrier only drops below the conrotatory ring closing barrier when the absolute barriers for ring closing are 2-4 kcal/mol (see ESI), and the timescale for closing would be on the order of ps. It seems possible to us that the timescale of force dissipation could be similar. In distinguishing between these possibilities, we note that the branching fraction obtained from molecular dynamics simulations (4.75 ± 2%) agrees well with the experimental results (5.0 ± 0.5%), and in those simulations the force is released instantly. That agreement suggests that the reaction inertia effects might be more significant.

Finally, we note that when the force disappears, a substantial amount of energy stored in enthalpic distortions of the polymer is released. That energy is initially transferred into kinetic energy of the atoms along the polymer backbone. In other words, the diradicaloid emerges from the release of force "hot," and ring closing might occur so quickly that the energy is not redistributed into the surrounding. As a consequence, the effective temperature of the reactant at which the ring closing occurs might be substantially higher than the temperature of the solvent, and that temperature might contribute to the reduced selectivity.

Conclusions

The approach described here expands the utility of mechanochemical methods as a tool for reaction engineering,[11,28-32] and it provides a rare experimental probe of the dynamics that can be simulated computationally in the vicinity of transition states, a topic that has received considerable attention recently. Interest is particularly high in the case of post-transition-state bifurcation,[33,34] conceptually similar to the behavior characterized here. In the case of the tension trapped diradicaloid, a significant (~5.0%) fraction of the released transition states surmount an additional reaction barrier of approximately 4 kcal/mol[15] (conrotation along the symmetry "forbidden" conrotatory pathway) or 6.6 kcal/mol (monorotation),[18] rather than taking the barrierless or

nearly barrierless trajectory down the symmetry allowed conrotatory ring closing.

The details that lead to those dynamics remain somewhat speculative, but at a minimum the results obtained here suggest that the *s-trans*/*s-trans* 1,3-diradicaloid transition state of the disrotatory ring opening is a competent intermediate structure along the *cis*-to-*trans* isomerization pathway; a given reaction trajectory might

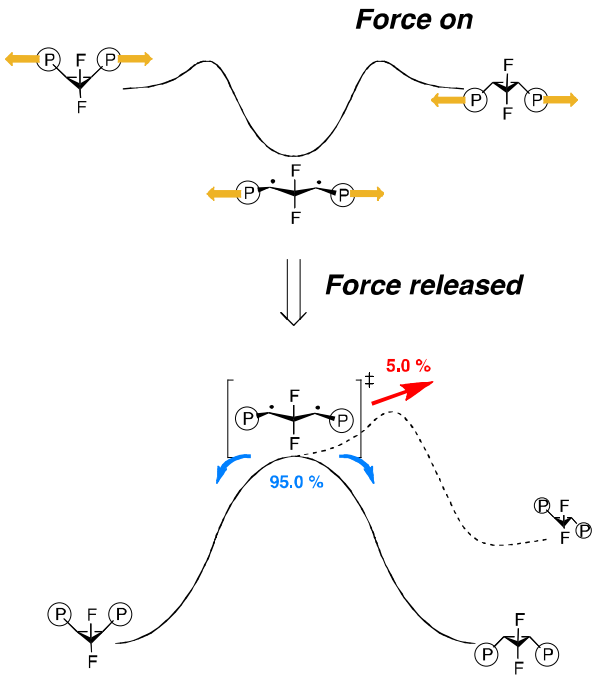

Figure 3. Ring-closing dynamics of a freed tension trapped transition state. Under tension applied by mechanochemical polymer extension (top), the 1,3-diradicaloid is trapped as a global minimum on the reaction potential energy surface. When the tension is released (bottom), the same diradicaloid structure is now the transition state along the force-free isomerization pathway of *cis*-*g*DFCs, but 5.0 ± 0.5% of the released structures surmount a nearby, additional barrier and close instead to the *trans* isomer. Note that the *trans* isomer could be formed from either direct conrotatory ring closing or a net conrotatory ring closing via sequential monorotation followed by disrotatory ring closing. The enantiomeric conrotatory closing and monorotatory pathways are not shown for clarity.

pass through both dividing surfaces, rather than immediately rolling energetically downhill after surmounting the first summit. The relatively high level of branching to the conrotatory pathway also raises the intriguing possibility that more subtle dynamical contributions might be at play in tension trapping, for example those due to competition between relaxation of the previously overstrained conformations (i.e., the rate at which the force goes to zero) and the dynamics of nuclear motion along the available reaction coordinates. Further characterization of the ultrafast dynamics at play in this and related systems might offer promise not only in testing fundamental notions of reaction dynamics, but offer an opportunity through which to steer the outcomes of chemical reactions toward unconventional products.

Experimental Section

Synthesis

Unless otherwise stated, all starting materials and reagents were purchased from Sigma-Aldrich and used as received. $CDCl_3$ was purchased from Cambridge Isotope Laboratory. Bromodifluoroacetic acid was purchased from SynQuest Laboratory. Dichloromethane (DCM) was purchased from VWR. For detailed synthetic procedures, see SI.

Sonication

Sonication experiments were performed in inhibitor-free THF on a Vibracell Model VCX 500 operating at 20 kHz with a 12.8 mm titanium tip probe from Sonics and Materials (http:www.sonics.biz/). Each sonication was performed on 1 mg/mL polymer solution in ~ 15 mL of THF. Prior to sonication, the solution was transferred to a 3-neck Suslick cell in an ice bath and deoxygenated by bubbling through nitrogen for 30 minutes. Irradiations were performed at 11.9 W/cm2 with a pulse sequence of 1s on/1s off while maintaining a temperature of 6-9 °C under a nitrogen atmosphere.

Characterization

^{1}H-NMR, ^{13}C-NMR, and ^{19}F-NMR analysis were conducted on a 400 MHz Varian spectrophotometer and the residual solvent peaks ($CDCl_3$ 7.26 ppm [1H], 77.16 ppm [13C]) were used as an internal chemical shift reference. ^{19}F spectra were indirectly referenced via the deuterium lock signal of $CDCl_3$ using the respective reference frequencies ratio as recommended.[35] All chemical shifts are given in ppm (δ) and coupling constants (J) in Hz as singlet (s), doublet (d), triplet (t), quartet (q), multiplet (m), or broad (br).

Gel permeation chromatography (GPC) experiments were performed on an in-line two columns (Agilent Technology PL gel, 10^4 and 10^3 Å) using THF (inhibitor free) as the eluent. Molecular weights were calculated using a Wyatt Dawn EOS multi-angle light scattering (MALS) detector and Wyatt Optilab DSP Interferometric Refractometer (RI). The refractive index increment (dn/dc) values were determined by online calculation using injections of known concentration and mass.

ASSOCIATED CONTENT

Supporting Information. Synthetic details; NMR and GPC-MALS data; calculation of ring opening forces during sonication. This material is available free of charge via the Internet at http://pubs.acs.org.

AUTHOR INFORMATION

Corresponding Authors

todd.martinez@stanford.edu
stephen.craig@duke.edu

Notes

The authors declare no competing financial interest.

ACKNOWLEDGMENT

This material is based on work supported by the U.S. Army Research Laboratory and the Army Research Office under Grant W911NF-07-0409. Part of this work was performed under the auspices of the U.S. Department of Energy by Lawrence Livermore National Laboratory under Contract DE-AC52-07NA27344.

REFERENCE

(1) Arrowsmith, P.; Bartoszek, F. E.; Bly, S. H. P.; Carrington, T.; Charters, P. E.; Polanyi, J. C. *J. Chem. Phys.* **1980**, *73*, 5895.
(2) Hering, P.; Brooks, P. R.; Curl, R. F.; Judson, R. S.; Lowe, R. S. *Phys. Rev. Lett.* **1980**, *44*, 687.
(3) Zewail, A. H. *Science* **1988**, *242*, 1645.
(4) Neumark, D. M. *Annu. Rev. Phys. Chem.* **1992**, *43*, 153.
(5) Wenthold, P. G.; Hrovat, D. A.; Borden, W. T.; Lineberger, W. C. *Science* **1996**, *272*, 1456.
(6) Ribas-Arino, J.; Marx, D. *Chem. Rev. (Washington, DC, U. S.)* **2012**, *112*, 5412.
(7) Caruso, M. M.; Davis, D. A.; Shen, Q.; Odom, S. A.; Sottos, N. R.; White, S. R.; Moore, J. S. *Chem. Rev. (Washington, DC, U. S.)* **2009**, *109*, 5755.
(8) Beyer, M. K.; Clausen-Schaumann, H. *Chem. Rev. (Washington, DC, U. S.)* **2005**, *105*, 2921.
(9) Liang, J.; Fernandez, J. M. *ACS Nano* **2009**, *3*, 1628.
(10) Wu, D.; Lenhardt, J. M.; Black, A. L.; Akhremitchev, B. B.; Craig, S. L. *J. Am. Chem. Soc.* **2010**, *132*, 15936.
(11) Hickenboth, C. R.; Moore, J. S.; White, S. R.; Sottos, N. R.; Baudry, J.; Wilson, S. R. *Nature* **2007**, *446*, 423.
(12) Yang, Q.-Z.; Huang, Z.; Kucharski, T. J.; Khvostichenko, D.; Chen, J.; Boulatov, R. *Nat Nano* **2009**, *4*, 302.
(13) Sheiko, S. S.; Sun, F. C.; Randall, A.; Shirvanyants, D.; Rubinstein, M.; Lee, H.-i.; Matyjaszewski, K. *Nature* **2006**, *440*, 191.
(14) Basedow, A. M.; Ebert, K. H. *Advanced Polymer Science* **1977**, *22*, 83.
(15) Lenhardt, J. M.; Ong, M. T.; Choe, R.; Evenhuis, C. R.; Martinez, T. J.; Craig, S. L. *Science* **2010**, *329*, 1057.
(16) Klukovich, H. M.; Kean, Z. S.; Ramirez, A. L. B.; Lenhardt, J. M.; Lin, J.; Hu, X.; Craig, S. L. *J. Am. Chem. Soc.* **2012**, *134*, 9577.
(17) Lenhardt, J. M.; Ogle, J. W.; Ong, M. T.; Choe, R.; Martinez, T. J.; Craig, S. L. *J. Am. Chem. Soc.* **2011**, *133*, 3222.
(18) Tian, F.; Lewis, S. B.; Bartberger, M. D.; Dolbier, W. R.; Borden, W. T. *J. Am. Chem. Soc.* **1998**, *120*, 6187.
(19) Getty, S. J.; Hrovat, D. A.; Xu, J. D.; Barker, S. A.; Borden, W. T. *J. Chem. Soc., Faraday Trans.* **1994**, *90*, 1689.
(20) Hillmyer, M. A.; Laredo, W. R.; Grubbs, R. H. *Macromolecules* **1995**, *28*, 6311.
(21) Kuijpers, M. W. A.; Iedema, P. D.; Kemmere, M. F.; Keurentjes, J. T. F. *Polymer* **2004**, *45*, 6461.
(22) Lenhardt, J. M.; Black, A. L.; Craig, S. L. *J. Am. Chem. Soc.* **2009**, *131*, 10818.
(23) Lenhardt, J. M., Duke University, 2011.
(24) Wang, J.; Kouznetsova, T. B.; Niu, Z.; Ong, M. T.; Klukovich, H. M.; Rheingold, A. L.; Martinez, T. J.; Craig, S. L., *Submitted*.
(25) Ong, M. T.; Leiding, J.; Tao, H. L.; Virshup, A. M.; Martinez, T. J. *J. Am. Chem. Soc.* **2009**, *131*, 6377.
(26) Carpenter, B. K. *J. Am. Chem. Soc.* **1996**, *118*, 10329.
(27) Hrovat, D. A.; Fang, S.; Borden, W. T.; Carpenter, B. K. *J. Am. Chem. Soc.* **1997**, *119*, 5253.
(28) Piermattei, A.; Karthikeyan, S.; Sijbesma, R. P. *Nature Chem.* **2009**, *1*, 133.
(29) Wiggins, K. M.; Hudnall, T. W.; Shen, Q.; Kryger, M. J.; Moore, J. S.; Bielawski, C. W. *J. Am. Chem. Soc.* **2010**, *132*, 3256.
(30) Kean, Z. S.; Niu, Z.; Hewage, G. B.; Rheingold, A. L.; Craig, S. L. *J. Am. Chem. Soc.* **2013**, *135*, 13598.
(31) Larsen, M. B.; Boydston, A. J. *J. Am. Chem. Soc.* **2013**, *135*, 8189.
(32) Tian, Y.; Kucharski, T. J.; Yang, Q. Z.; Boulatov, R. *Nat. Commun.* **2013**, *4*.
(33) Ess, D. H.; Wheeler, S. E.; Iafe, R. G.; Xu, L.; Celebi-Olcum, N.; Houk, K. N. *Angew. Chem., Int. Ed.* **2008**, *47*, 7592.
(34) Hong, Y. J.; Tantillo, D. J. *Nature Chem.* **2014**, *6*, 104.
(35) Harris, R. K.; Becker, E. D.; De Menezes, S. M. C.; Goodfellow, R.; Granger, P. *Pure Appl. Chem.* **2001**, *73*, 1795.

Insert Table of Contents artwork here